PARAMETERIZATION OF DRAG COEFFICIENTS OVER POLAR SEA ICE FOR CLIMATE MODELS

By Christof Lüpkes[1] and Vladimir M. Gryanik[1,2]

[1] Alfred-Wegener-Institut Helmoltz-Zentrum für Polar- und Meeresforschung, Bremerhaven, Germany
[2] A.M. Obukhov Institute of Atmospheric Physics, Russian Academy of Sciences, Moscow, Russia.

Proof of publication in: Mercator Ocean Quarterly Newsletter - Special Issue with ICE-ARC No 51 March 2015, 29-34

Abstract

A parameterization of drag coefficients has been developed in recent years that accounts for the impact of edges at ice floes, leads, and melt ponds on momentum transport. Melt ponds are a common feature in the inner Arctic during summer while drifting ice floes and their edges influence the surface roughness especially in the marginal sea ice zones during all seasons. Governing parameters in the parameterization that can be easily applied to climate models are the sea ice concentration and aspect ratio h/D where h is the ice freeboard and D is the characteristic length of floes and ponds/leads. When these parameters are not available from a sea ice model, the aspect ratios can also be parameterized as a function of the sea ice concentration so that the new schemes can also be used in stand-alone atmospheric models using observed sea ice concentration. The parameterization is evaluated for idealized meteorological forcing and prescribed sea ice and melt pond concentration in the Siberian Arctic and in parts of the Central Arctic. The required sea ice data are available from remote sensing. The distributions of drag coefficients obtained from traditional parameterizations and from the new one show large differences in this test scenario especially in the region south of 80°N.

Introduction

Neutral drag coefficients observed over polar sea ice show a large variability with values roughly between 0.5×10^{-3} and 4×10^{-3} (Anderson, R.J., 1987; Andreas et al., 1984; Overland, 1985; Fairall and Markson, 1987; Guest and Davidson, 1987; Hartmann et al., 1994; Kottmeier et al., 1994; Mai et al., 1996; Garbrecht et al., 2002; Schröder et al., 2003). This variability is caused by the inhomogeneous sea ice surface topography which is a result of convergent and divergent sea ice drift causing the formation of ridges, small floes and leads. Also melting processes influence the sea ice topography due to the formation of melt ponds and related edges.

There have been many attempts in the past to parameterize the sea ice roughness with various concepts. The focus here is on schemes that distinguish between skin drag, related to the relatively smooth surface of level ice, and form drag caused by the edges of the ridges, floes and melt ponds. Such schemes have been developed especially for the marginal sea ice zones (MIZ) where the variability of roughness is mainly caused by the inhomogeneous distribution of floe edges (Hanssen-Bauer and Gjessing, 1988; Mai et al., 1996; Stössel and Claussen,1993; Steiner (2001), Birnbaum and Lüpkes, 2002; Lüpkes and Birnbaum, 2005). Since the number density of edges is connected with the sea ice concentration A, the latter can be used as a dominating parameter for the drag coefficients.

The dependence on A has been shown by Andreas et al. (2010) on the basis of measured drag coefficients also for the inner Arctic during summer when leads and melt ponds have formed. They proposed a quadratic dependence of the neutral 10 m drag coefficient C_{dn10} on A which resulted from a fit to drag coefficients derived from in-situ turbulence data over the Beaufort Sea and the marginal sea ice zone. In typical conditions results of this fit do not differ much from the results of the more complex parameterizations mentioned above. Thus this approach can be considered as a progress and it shows furthermore that the A related parameterization of C_{dn10} is possible in a much larger region than the MIZ. The drawback is, however, that this approach does not allow the adjustment of the drag coefficients to variable sea ice topography and does not allow coupling with the usual wind speed dependent parameterizations of the drag coefficients over water, which should be possible at least for small sea ice cover.

A further step followed by Lüpkes et al. (2012) (LU12). They showed that the quadratic fit proposed by Andreas et al. (2010) can be obtained as a special case of the above mentioned more general and physically based drag partitioning concept, when this is extended e.g. to include also inner Arctic conditions and when certain simplifying assumptions are made. The LU12 parameterization will be explained and discussed in section 2. It includes the dependence of drag coefficients on sea ice topography parameters and allows the formulation of the required neutral drag coefficients for sea ice models. Lüpkes and Gryanik (2015) included later the dependence of drag coefficients on stability which is explained here in its lowest level of complexity.

In sections 3 and 4, we show practical consequences of the new parameterization by comparing its results with those of a typical parameterization used currently in climate models.

Form drag dependent parameterization of momentum fluxes

The concept of drag partitioning together with flux averaging results in the effective neutral drag coefficients over a surface consisting of water and ice of concentration A so that:

$$C_{dn10} = C_{dn10,w}\,(1-A) + C_{dn10,i}\;A + C_{dn10,f}\;, \qquad (1)$$

where $C_{dn10,w}$ and $C_{dn10,i}$ are the neutral skin drag coefficients over water and ice at 10 m height and $C_{dn10,f}$ is the form drag coefficient for neutral stratification. Applying some algebra, LU12 proved that this approach (1) is equivalent with the Andreas et al. (2010) fit when fixed values are prescribed for $C_{dn10,w}$ and $C_{dn10,i}$ and when $C_{dn10,f}$ is proportional to A (1-A). Since the latter cannot be expected in general, LU12 investigated also whether this kind of A dependence exists in special conditions. To that aim, they derived first $C_{dn10,f}$ by calculating the dynamic pressure against floe edges similarly as proposed already by Hanssen-Bauer and Gjessing (1988) and by Arya (1975) (but now in 3D formulation and using less restrictive assumptions). They arrived finally at:

$$C_{dn10,f} = (c_e/2)\;[\,\ln(h_f / z_{0w}) / \ln(10/e\; z_{0w})\,]^2\;(S_c)^2\;(h_f / D_i)\;A \qquad \text{(MIZ)} \qquad (2)$$

$$C_{dn10,f} = (c_e/2)\;[\,\ln(h_p / z_{0w}) / \ln(10/e\; z_{0w})\,]^2\;(S_c)^2\;(h_p / D_w)\;(1-A)\;, \qquad \text{(inner Arctic)} \qquad (3)$$

where e = 2.718 is the Eulerian constant and all units of parameters are in meters. z_{0w} and z_{0i} are the skin drag related roughness lengths over open water and sea ice, h_f is the sea ice freeboard of drifting floes in the MIZ, h_p is the freeboard of ice related to the water surface in melt ponds/leads. D_i and D_w are the diameters of floes and ponds/leads and S_c are functions accounting for the sheltering of wind by ice floes. They can be set either to 1 or can be parameterized in terms of A in the simplest cases (see LU12). c_e is a constant that contains the coefficient of resistance of an individual roughness element, and that accounts for the floe and pond geometry (its deviation from a circular shape). For simplicity, we use the same letter for drag coefficients in the MIZ and inner Arctic and do the same for the sheltering functions although they differ from each other in general.

It is remarkable that the dependence of the drag coefficients in equations (2) and (3) on the sea ice concentration is different in both sea ice regimes. The reason is that there are differences between both morphologies. For example, sea ice floes appear to be disconnected in the MIZ case (at least for moderate values of the sea ice concentration) while the ice areas surrounding ponds are approximately connected. A further difference is that edges have a concave shape in the case of melt ponds and a convex one in the case of floes in the MIZ with regard to the upstream flow. Hence the formulae for the inner Arctic and MIZ differ in this general form from each other and differ a lot also from the AN10 quadratic fit that is proposed for both regions.

In the form (2) and (3) the parameterization can be applied to ocean or atmosphere models when they are coupled with a sea ice model providing the topography parameters. While these models provide h_f and h_p which are connected with the sea ice thickness, it is more difficult to obtain D_i and D_w. This problem has been solved by LU12 by showing that the latter two parameters, and in the most simplified level of the parameterization also h_f and h_p, can be parameterized as a function of the sea ice concentration. To that aim they used satellite observations of melt ponds (Fetterer et al., 2008) and aircraft observations of floe parameters over the MIZ from the campaigns REFLEX (Hartmann et al., 1994; Mai et al., 1996).

Inserting these parameterizations and using typical values for the roughness lengths, LU12 obtained the formulation:

$$C_{dn10,f} = C\ A\ (1-A)^{\beta} \qquad (4)$$

It is valid for both MIZ and inner Arctic with ponds/leads but with different values of constants (MIZ: $C = 3.67 \times 10^{-3}$, $\beta = 1.4$; inner Arctic: $C = 2.23 \times 10^{-3}$, $\beta = 1.1$). The scatter of observed topography parameters around the parameterized curves (see LU12) suggests that the parameters β and C should not be considered as fixed values. We expect that the possible ranges are large with $1.3 \times 10^{-3} < C < 4.5 \times 10^{-3}$ and $0.3 < \beta < 1.8$ so that this range is allowed for sensitivity studies aiming at an improved understanding of the ice-air-ocean interaction processes.

The functional dependence on A which is required for the analogy to the Andreas et al. (2010) fit is approximately obtained by (4) using the given values for C and β for the inner Arctic, and it is exactly obtained for $\beta = 1$. It has to be stressed, however, that this equivalence is obtained only under restrictive assumptions ignoring, for example, that aspect ratios can vary also for fixed values of A, and also that in general, for example h_p and D_w depend in a more complex way on A than was assumed to obtain (4). For this reason, the parameterization (1) with (2) and (3) should be chosen when the topography parameters are available from sea ice models, and equation (1) with (4) is appropriate in stand-alone-atmosphere models. We will refer to the latter as the AWI parameterization in the following.

There is one further aspect of the parameterization that was considered by Lüpkes et al. (2013). This concerns the definition of A. In previous parameterizations melt ponds have never been considered as a source of roughness. Since this is different for equations (2), (3) and (4), A has to be redefined not as the sea surface related ice fraction A_{SSI} as usually done, but as the ice surface related fraction so that $A = A_{SSI} - A_p$ where A_p is the fraction of ponds on floes in a grid cell. The relevance of this change is explained in the next section.

Equations (1) with (4) give the effective drag coefficient for a grid cell with open water and sea ice. However, in models using flux averaging, the fluxes have to be separated into a contribution over open water and another one over sea ice. The latter contribution is needed also in sea ice models. Form drag modifies the fluxes over ice only so that the effective drag coefficient over ice is obtained as:

$$C_{dn10,i,eff} = C_{dn10,i} + C_{dn10,f} / A \quad . \qquad (5)$$

Since in (4) β is only slightly different from 1 in the inner Arctic, equation (5) shows that in this case $C_{dn10,i,eff}$, which is needed to calculate the momentum flux per unit ice area, depends quasi linearly on A. We stress that this dependence holds only when the large simplifications described above are carried out. In general, however, the dependence is nonlinear and this holds also for the effective drag coefficient C_{dn10} over the mixture of ice and open water (equation (1) with (4)).

Results of neutral drag coefficients for different scenarios

For simplicity, we discuss in the following only results obtained with the AWI parameterization (equation (1) with (4)) and compare them with results of parameterizations used for some state-of-the art climate models (ECHAM5/6, Roeckner et al., 2003; Giorgetta et al., 2012; CAM5, Neale et al., 2010) and for the momentum forcing of the ocean model MITgcm (Marshall et al., 1997). In these parameterizations only skin drag (equation 1 with $C_{dn10,f} = 0$) is considered. We start with Figure 1 showing observations versus results of the parameterizations. Observed data result from aircraft observations (REFLEX) mentioned above and from the SHEBA campaign (ASFG tower) as analyzed by Andreas et al. (2010). Prior to 2013 effective drag coefficients used in GCMs depended linearly on A and form drag was included implicitly in the parameterizations by adjusting $C_{dn10,i}$ to high values. This contrasts with the results of the AWI parameterization and with measurements showing a nonlinear dependence on A.

Figure 1:

As a first test, Lüpkes et al. (2013) used the AWI parameterization to calculate the distribution of drag coefficients over the whole Arctic Ocean for prescribed homogeneous wind speed and compared the results with those from the parameterizations used in the GCMs considered above. Large differences were found for the general Arctic-wide distribution of the drag coefficients. Compared with the new parameterization the traditional parameterizations underestimated the drag coefficients in the regions with large melt pond cover and lead fraction (e.g. in the Beaufort Sea region).

Figure 2:

We consider in Figure 2 results of a similar study, but now only for a selected region in the Eastern Arctic (Siberian Sea, Laptev Sea, part of Central Arctic). Neutral drag coefficients are shown which were obtained with the ECHAM5/6 parameterization and with the AWI parameterization (equation 1 with 4 using parameter values for the inner Arctic). Sea ice and melt pond fraction were provided from the *Integrated Climate Data Center (ICDC), CliSAP/KlimaCampus, University of Hamburg, Germany (http://icdc.zmaw.de)* (see also Rösel et al., 2012). It can be seen that the largest differences between both parameterizations occur in the region south of 80°N. There, the large melt pond cover causes an increase of form drag and thus increases the drag coefficients obtained with the AWI parameterization. On the contrary, drag coefficients obtained with the ECHAM parameterization decrease in this region relative to the values north of 80°N since only skin drag is considered and due to the differences in the ice concentration variables A_{SSI} used in the traditional parameterization and A_{SSI}-A_p used in the AWI parameterization.

Generalized AWI parameterization for stability dependent drag coefficients

Sea ice covered regions are often characterized by strongly stable stratification of the atmospheric boundary layer. Furthermore, especially during winter, large differences can occur between the stratification over ice and open water so that the stability dependence of drag coefficients has to be taken into account in the parameterization. For this reason Lüpkes and Gryanik (2015) formulated a parameterization of the form drag coefficient which is similar to equations (2) and (3) but accounts for the fetch and stability dependence of wind on the upstream side of floe, melt pond, and lead edges. In its most simplified level, the stability dependent form drag coefficient at 10 m height is given by:

$$C_{d10,f} = C_{dn10,f} [(1-A) f_{m,w} + A f_{m,i}] , \quad (6)$$

where $f_{m,w}$ and $f_{m,i}$ are stability correction functions over open water (w) and ice (i), formulated in terms of Monin-Obukhov theory or applying the Louis (1979) concept as a function of the bulk Richardson numbers over ice and open water. In this level $C_{dn10,f}$ is again given by equation (4) but with slightly modified values of the constant C (for summer: C = 2.20, for the MIZ: C = 3.54).

Roughness elements like floe edges increase the mechanical turbulence which also influences the heat flux. Thus a parameterization corresponding to (4) and (6) was derived by Lüpkes and Gryanik (2015) also for the heat transfer coefficient which is not discussed further here, but which should be used together with the stability dependent parameterization of the form drag.

To get an impression of the stability impact we show as a test of the parameterization results in Figures 3 and 4 for C_{d10} (equation 1 with 4 and 6) for idealized cases of warm air advection. In one case, the air is prescribed to be warmer than the ice and water surface (Figure 3), in a second case, the air temperature is still warmer than the ice surface, but colder than the water surface (Figure 4). For the test, we prescribed in the whole area constant values for the wind speed and for the air and surface temperatures of ice and water. The used values (see figure caption) can occur during summer over large parts of the Arctic. The stability functions $f_{m,w}$ and $f_{m,i}$ have been calculated using the Louis (1979) concept as in ECHAM6 (Giorgetta et al., 2012) and in the coupled model ECHAM6-FESOM (Sidorenko et al., 2014). A comparison of the drag coefficients with Figure 2 for neutral conditions shows the strong impact of stability although we considered cases with only small deviations from neutral stratification. In the region with large melt pond cover (south of 80°N) drag coefficients obtained with the AWI parameterization decrease slightly in the stable case, but they increase strongly in the unstable case. Obviously, the new parameterization reacts stronger than the ECHAM6 parameterization on small changes in stability which leads to the asymmetric response in the shown cases. As for neutral conditions, differences between the ECHAM6 parameterization and the AWI parameterization are also largest south of 80°N. Lüpkes et al. (2015) show furthermore that the sea ice concentration, for which the drag coefficients attain their maximum values, depends on the stability and that this dependence differs in the new and traditional parameterizations as can be seen also in the present figures. Thus the new schemes might help to better understand momentum exchange between air and sea ice and related effects in a changing climate with changing temperature conditions and sea ice concentration.

Figure 3:

Figure 4:

Conclusions

The interaction between atmosphere, sea ice, and ocean depends strongly on the transfer coefficients for momentum and heat. Observations show that in regions with fractional sea ice cover the neutral transfer coefficients for momentum are closely linked with the sea ice concentration A and that they depend nonlinearly on A. Parameterizations of the momentum transfer coefficients reproduce the observed nonlinearity when a concept is used that distinguishes between skin drag over level ice and open water and form drag caused by the edges of floes, melt ponds and leads. A parameterization of the drag coefficients and their stability dependence by Lüpkes et al. (2012) and Lüpkes and Gryanik (2015) is available for climate models in different complexity levels. The most complex level can be used when sea ice topography parameters are known from a sea ice model, the lowest level is appropriate for a stand-alone atmospheric model using sea ice concentration e.g. from reanalysis.

Results have shown that the new parameterization has a large impact on drag coefficients especially in regions with large melt pond and lead cover such as in the Beaufort Sea and Siberian Sea regions. This holds especially when the stabilities over ice and open water differ from each other since form drag is influenced by both stabilities due to the fetch dependence of the wind profiles. Beyond the simple test cases shown in Figures 2, 3, and 4 the parameterizations should be implemented in climate models to better understand their role for ice-atmosphere interaction processes.

The new parameterizations have been developed following the traditional line including the effect of sea ice pressure ridges in the skin drag coefficient over ice. A possible extension of our approach to include the effect of ridges in the form drag coefficient was suggested by Tsamados et al. (2014) and by Castellani et al (2014).

Acknowledgments

We thank E.L Andreas for providing measured drag coefficients from SHEBA, J. Hartmann for data from the marginal sea ice zones (REFLEX), and L. Kaleschke for sea ice and melt pond data. We further thank E.L Andreas, J. Hartmann, G. Birnbaum W. Dorn, D. Sein, and D. Sidorenko for helpful discussions. This work contributes to the project MiKlip funded by the German Federal Ministry of Education and Research (FKZ: 01LP1126A).

References

Anderson, R.J. 1987: Wind stress measurements over rough sea ice during the 1984 Marginal Ice Zone Experiment, J. Geophys. Res. 92(C7): 6933–6941.

Andreas, E.L, Horst, T.W., Grachev, A.A., Persson, P.O.G., Fairall, C.W., Guest, P.S. and Jordan, R.E. 2010: Parametrizing turbulent exchange over summer sea ice and the marginal ice zone, Q.J.R. Meteorol. Soc.138: 927–943.

Andreas, E.L,Tucker III, W.B. and Ackley S.F. 1984: Atmospheric boundary-layer modification, drag coefficient, and surface heat flux in the Antarctic marginal ice zone, J. Geophys. Res. 89(C1): 649-661.

Arya, S.P.S. 1975: A drag partitioning theory for determining the large-scale roughness parameter and wind stress on the Arctic pack ice, J. Geophys. Res. 80, No 24: 3447-3454.

Birnbaum, G., and Lüpkes, C. 2002: A new parametrization of surface drag in the marginal sea ice zone, Tellus, Ser. A 54(1): 107–123.

Castellani, G., Lüpkes, C. Hendricks, S. and Gerdes, R. 2014: Variability of Arctic sea-ice topography and its impact on the atmospheric surface drag, J. Geophys. Res. Oceans119, doi:10.1002/2013JC009712.

Fairall, C.W. and Markson R. 1987: Mesoscale variations in surface stress, heat fluxes, and drag coefficient in the marginal ice zone during the 1983 marginal ice zone experiment, J. Geophys. Res. 92: 6921-6932.

Fetterer, F., Wilds, S. and Sloan, J. 2008: Arctic sea ice melt pond statistics and maps, 1999–2001, http://nsidc.org/data/docs/noaa/g02159_ponds/index.html, Natl. Snow and Ice Data Cent., Boulder, Colo.

Garbrecht, T., Lüpkes, C., Hartmann, J. and Wolff, M. 2002: Atmospheric drag coefficients over sea ice-Validation of a parametrisation concept, Tellus A 54(2): 205-219.

Giorgetta, M.A., et al. 2012: The atmospheric general circulation model ECHAM6. Model description, Max Planck Inst. for Meteorol., Hamburg, Germany, 27 September 2012, 156 pp.

Guest, P. S. and Davidson, K.L. 1987: The effect of observed ice conditions on the drag coefficient in the summer East Greenland Sea marginal ice zone, J. Geophys. Res. 92(C7): 6943-6954.

Hanssen-Bauer, I. and Gjessing Y.T. 1988: Observations and model calculations of aerodynamic drag on sea ice in the Fram Strait, Tellus, Ser. A, 40: 151-161.

Hartmann, J., Kottmeier,C., Wamser, C. and E. Augstein 1994: Aircraft measured atmospheric momentum, heat and radiation fluxes over Arctic sea ice, in The Polar Oceans and Their Role in Shaping the Global Environment, Geophys. Monogr. Ser., vol. 85, edited by O. M. Johannessen, R. D. Muench, and J. E. Overland, AGU, Washington, D. C.: 443-454.

Kottmeier, C., Hartmann, J. Wamser, C., Bochert, A., Lüpkes, C., Freese, D. and Cohrs, W. 1994: Radiation and eddy flux experiment 1993 (REFLEX II), Rep. Polar Res. 133, 62 pp., Alfred Wegener Inst., Bremerhaven, Germany.

Louis, J. F. (1979), A parametric model of vertical eddy fluxes in the atmosphere, *Boundary Layer Meteorol.*, *17*, 187–202.

Lüpkes, C. and Gryanik, V.M. 2015: A stability dependent parametrization of transfer coefficients for momentum and heat over polar sea ice to be used in climate models, *J. Geophys. Res. Atmos.*, *120*, doi:10.1002/2014JD022418.

Lüpkes, C., Gryanik, V.M., Rösel, A., Birnbaum, G. and Kaleschke, L. 2013: Effect of sea ice morphology during Arctic summer on atmospheric drag coefficients used in climate models, Geophys. Res. Lett., 40: 446-451, doi:10.1002/grl.50081.

Lüpkes, C., Gryanik, V.M., Hartmann, J. and Andreas E.L 2012: A parametrization, based on sea ice morphology, of the neutral atmospheric drag coefficients for weather prediction and climate models, J. Geophys. Res., 117, D13112, doi:10.1029/2012JD017630.

Lüpkes, C. and Birnbaum, G. 2005: Surface drag in the Arctic marginal sea-ice zone: A comparison of different parameterisation concepts, Boundary Layer Meteorol. 117: 179-211.

Mai, S., Wamser, C. and Kottmeier, C. 1996: Geometric and aerodynamic roughness of sea ice, Boundary Layer Meteorol. 77: 233-248.

Marshall, J., Adcroft, A., Hill, C., Perelman, L. and Heisey C. 1997: A finite-volume, incompressible Navier–Stokes model for studies of the ocean on parallel computers, J. Geophys. Res., 102(C3): 5753-5766.

Neale, R.B., Gettelman, A., Park, S., Conley, A.J., Kinnison, D., Marsh, D., Smith, A.K., Vitt, F., Morrison, H., Cameron-Smith, P., Collins, W.D., Iacono, M.J., Easter, R.C., Liu, X. and Taylor, M.A. 2010: Description of the NCAR Community Atmospheric Model (CAM 5.0), NCAR technical note, NCAR/TN-486 + STR, 268 pp.

Nguyen T., Menemenlis, D. and Kwok, R. 2011: Arctic ice-ocean simulation with optimized model parameters: Approach and assessment, J. Geophys. Res., 116, C04025, doi:10.1029/2010JC006573.

Overland, J. E. 1985: Atmospheric boundary layer structure and drag coefficients over sea ice, *J. Geophys. Res.*, *90*, 9029–9049.

Roeckner, E., Bäuml, G., Bonaventura, L, Brokopf, R., Esch, M., Giorgetta, M., Hagemann, S., Kirchner, I., Kornblueh, L, Manzini, E., Rhodin, A., Schlese, U., Schulzweida, U. and Tompkins, A. 2003: The atmospheric general circulation model ECHAM5. Part 1. Model description, *MPI Rep., 349*, Max Planck Inst. for Meteorol., Hamburg, Germany.

Rösel, A., Kaleschke, L. and Birnbaum, G. 2012: Melt ponds on Arctic sea ice determined from MODIS satellite data using an artificial neural network, The Cryosphere, 6, doi:10.5194/tc-6-431-2012.

Schröder, D., Vihma, T., Kerber, A. and Brümmer, B. 2003: On the parametrisation of turbulent surface fluxes over heterogeneous sea ice surfaces, J. Geophys. Res., 108(C6), 3195, doi:10.1029/2002JC001385.

Sidorenko, D., Rackow, T., Jung, T., Semmler, T., Barbi, D., Danilov, S., Dethloff, K., Dorn, W., Fieg, K., Gößling, H.F., Handorf, D., Harig, S., Hiller, W., Juricke, S., Losch, M., Schröter, J., Sein, D. and Wang, Q. 2014: Towards multi-resolution global climate modeling with ECHAM6-FESOM. Part I: Model formulation and mean climate, *Clim. Dyn*, doi:10.1007/s00382-014-2290-6.

Steiner, N. 2001: Introduction of variable drag coefficients into sea-ice models, Ann. Glaciol., 33, 181-186.

Stössel, A. and Claussen, M. 1993: On the momentum forcing of a largescale sea-ice model, Clim. Dyn. 9: 71-80.

Tsamados, M., D. L. Feltham, D. Schröder, D. Flocco, S. L. Farrell, N. Kurtz, S. W. Laxon and S. Bacon 2014: Impact of variable atmospheric and oceanic form drag on simulations of Arctic sea ice, *J. Phys. Oceanogr.*, *44*, 1329–1353, doi:10.1175/JPO-D-13-0215.1.

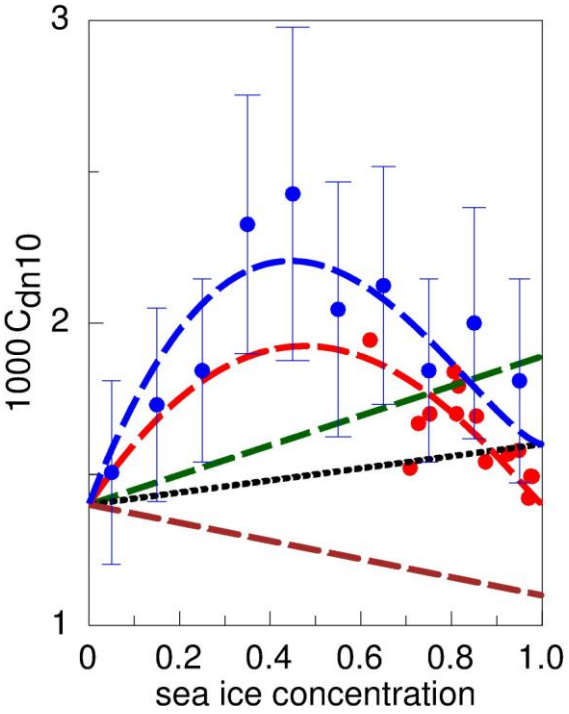

Figure 1: Neutral drag coefficients at 10 m height obtained from measurements (circles) and form parameterizations (lines). Red circles: Measurements over the Beaufort Sea (Andreas et al., 2010) and over the Fram Strait marginal sea ice zone (Hartmann et al. 1991, Mai et al., 1996). Red line: AWI parameterization (equation 1 with 4) for summer sea ice with ponds and leads. Blue line: AWI parameterization for MIZ conditions. Brown line: forcing suggested by Nguyen et al. (2011) for the MITgcm. Black dotted line: CAM5 parameterization. Green line: current ECHAM6 parameterization (see also text).

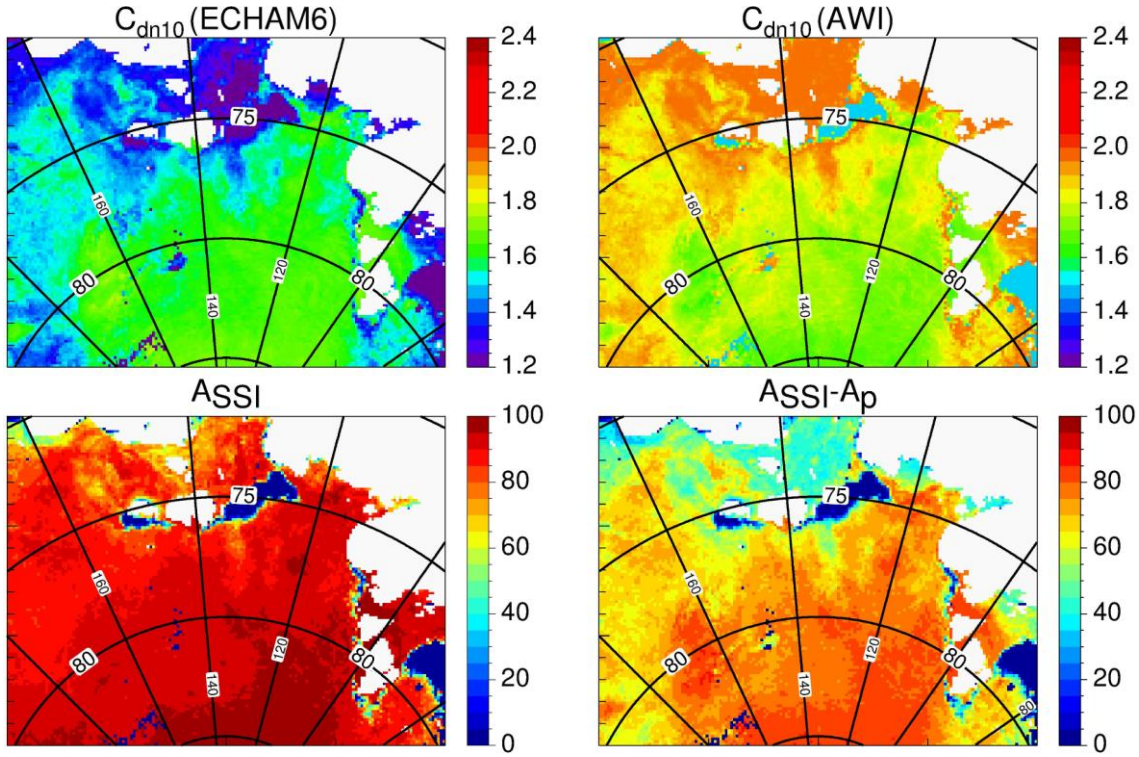

Figure 2: Neutral drag coefficients at 10 m height (C_{dn10}) obtained with the ECHAM6 parameterization and with the AWI parameterization (equation 1 with 4) over the Laptev Sea/East Siberian Sea and parts of the central Arctic. A_{SSI} is the sea ice concentration as used in current climate models e.g. in ECHAM6 (no melt ponds considered), $A_{SSI} - A_p = A$ is the sea ice concentration used in the AWI parameterization that accounts for melt ponds. A_p is the melt pond fraction. Sea ice and melt pond fraction represent a 1 week average in June 2004 and are based on remote sensing (see text).

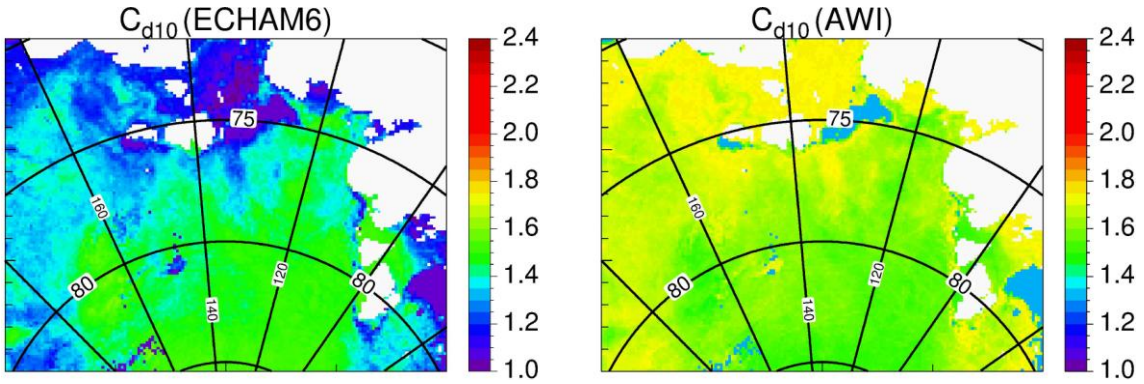

Figure 3: Drag coefficients at 10 m height (C_{d10}) obtained with the ECHAM6 parameterization and the AWI parameterization (equation 1 with 4 and 6). The same sea ice and melt pond data are used as in Figure 2 but the results represent a case with weak warm air advection and thus stable stratification over ice and water. Prescribed surface temperatures are 272.8 K over ice and 272.5 K over water. Air temperature is set to 273.5 K. Wind speed is 5 m/s. Ice concentration is prescribed as in Figure 2.

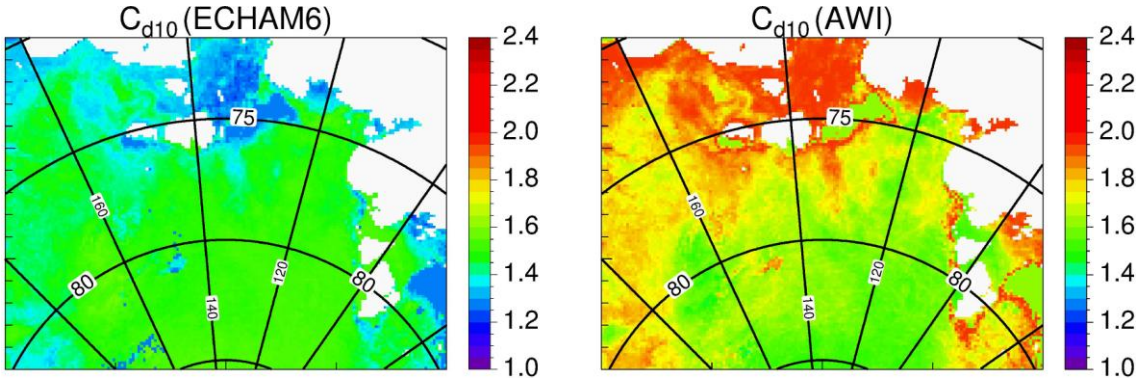

Figure 4: Same as Figure 3, but for a case with stable stratification over ice and unstable stratification over water. Surface temperature over water is set to 271.5 K and over ice to 268 K. Air temperature is 269 K. Ice concentration is prescribed as in Figure 2.